Frontiers in Bioscience Landmark

Front. Biosci. (Landmark Ed) **2026**; 31(1): 47950
https://doi.org/10.31083/FBL47950

Original Research

Turmeric-Derived Exosome-Like Nanoparticles Inhibit Non-Small Cell Lung Cancer via Epigenetic Regulation

Wenyu Sun[1,2], Da Liu[3,*], Zhenfa Zhang[1,*]

[1]Department of Lung Cancer Surgery, Tianjin Medical University Cancer Institute and Hospital, National Clinical Research Center for Cancer, Key Laboratory of Cancer Prevention and Therapy, Tianjin's Clinical Research Center for Cancer, 300060 Tianjin, China
[2]Department of Thoracic Oncology, Jilin Cancer Hospital, 130012 Changchun, Jilin, China
[3]Public Experimental Center, Changchun University of Chinese Medicine, 130017 Changchun, Jilin, China
*Correspondence: liuda@ccucm.edu.cn (Da Liu); zhangzhenfa@tmu.edu.cn (Zhenfa Zhang)
Academic Editor: Barbara Ruaro
Submitted: 3 November 2025 Revised: 2 December 2025 Accepted: 18 December 2025 Published: 8 January 2026

Abstract

Background: Turmeric-derived exosome-like nanoparticles (TELNs) are nanoscale vesicles of plant origin with therapeutic potential. However, the specific efficacy and mechanisms of TELNs in inhibiting non-small cell lung cancer (NSCLC) remain unclear. This study investigated the effects of TELNs on NSCLC by epigenetically regulatiing histone acetyltransferase human males absent on the first (hMOF) and histone H4K16 acetylation (H4K16ac). **Methods**: TELNs were isolated from turmeric using differential centrifugation and characterized by nanoparticle tracking analysis (NTA), transmission electron microscopy (TEM), and zeta potential measurements. Cellular uptake was assessed via PKH26 labeling. *In vitro* assays evaluated the effects of TELNs on apoptosis (annexin V/PI staining, JC-1 mitochondrial depolarization, caspase-3 cleavage) and proliferation (CCK-8). The *in vivo* efficacy of TELNs was examined in A549 xenografts. Bioinformatics and molecular docking analyses revealed the interaction of curcumin in TELNs with hMOF, while RNA interference validated the role of hMOF in TELN-mediated apoptosis and migration suppression. **Results**: TELNs exhibited exosome-shaped morphology and efficient uptake by A549 cells. Treatment with TELNs induced apoptosis and reduced tumor volume by 58.1%. Mechanistically, TELNs upregulated hMOF expression and H4K16ac levels. RNA interference confirmed that knockdown of hMOF weakened the effect of the TELNs. Molecular docking suggested curcumin in TELNs may interact with hMOF. **Conclusion**: This study reveals a novel epigenetic mechanism wherein TELNs suppress NSCLC by activating hMOF/H4K16ac. Curcumin within TELNs increases hMOF levels, thus positioning TELNs as a potential nanotherapeutics with the capacity for epigenetic modulation. Our findings underscore the potential of TELNs in NSCLC treatment and highlight hMOF as a therapeutic target.

Keywords: exosome; curcumin; non-small cell lung cancer; epigenesis; histone acetylation

1. Introduction

Non-small cell lung cancer (NSCLC) has the highest incidence and mortality rates of all cancer types [1]. Current therapeutic strategies include surgery and radiotherapy. However, surgical resection is unsuitable for frail patients, and incomplete tumor removal may lead to recurrence and metastasis. Radiotherapy induces tumor cell apoptosis by damaging DNA molecules via X-rays or proton beams [2]. However, it also exerts detrimental effects on adjacent healthy tissues and may cause pulmonary fibrosis in the long term [3]. Compared to conventional chemotherapeutic agents, natural products offer low toxicity, high biocompatibility, and the ability to suppress NSCLC through multi-pathway modulation [4].

Plant-derived exosome-like nanoparticles (PELNs) are nanoscale vesicles secreted by plant cells, ranging in diameter from 30 to 160 nm [5]. PELNs share structural similarities with mammalian exosomes, and their unique composition enhances antitumor efficacy [6]. These nanoparticles carry anti-cancer components such as microRNAs and flavonoids, significantly inhibiting tumor growth by inducing apoptosis and cell cycle arrest [7,8]. The phospholipid bilayer of PELNs maintains stability under physiological conditions and preserves biocompatibility benefits over synthetic nanocarriers [9]. Turmeric (*Curcuma longa L.*), a traditional Chinese herb, has been used historically to treat abdominal masses and malignancies [10]. Recent research attributes its anticancer properties to curdione and curcumin, which exhibit anti-metastatic and anti-angiogenic effects [11,12]. Yang *et al.* [13] successfully isolated turmeric-derived exosome-like nanoparticles (TELNs) and demonstrated their inhibitory effect on human colorectal cancer cells.

Although TELNs show potential for cancer treatment, their effects on NSCLC and the underlying mechanisms remain unclear. In this study, TELNs were successfully isolated, and their mechanism of action against NSCLC was demonstrated for the first time. Our results demonstrate that TELNs affect the expression and activity of the histone acetyltransferase hMOF. This subsequently increases the acetylation of histone H4 at lysine 16 (H4K16ac), thereby suppressing NSCLC epigenetically. We initially investi-

gated the *in vitro* and *in vivo* antitumor efficacy of TELNs, as well as the specific regulation of hMOF. Molecular docking also revealed the potential interaction between TELNs and hMOF. Our findings establish, for the first time, that TELNs exert anti-NSCLC effects via hMOF/H4K16ac-mediated epigenetic regulation. This provides a foundation for the use of natural nanoparticles to develop therapies based on epigenetic reprogramming.

2. Materials and Methods

2.1 Materials

Cell Counting Kit-8 (CCK-8, AC11L054) was purchased from Life-iLab Biotech Co., Ltd. (Shanghai, China). The Annexin V/PI staining kit (FAK012.20) was purchased from NeoBioscience Technology Co, Ltd. (Shenzhen, China). JC-1 staining kit (AC13021) was sourced from Acmec Biochemical Technology Co., Ltd. (Shanghai, China). The BCA kit was purchased from Beyotime Biotechnology Co., Ltd. (Shanghai, China). Dulbecco's Modified Eagle Medium (DMEM), Roswell Park Memorial Institute (RPMI) 1640 medium, fetal bovine serum (FBS) and trypsin were acquired from Gibco (USA). Anti-hMOF antibody (ab200660), anti-H4K16ac antibody (ab109463), anti-histone H4 antibody (ab7311), anti-procaspase-3 antibody (ab32150), and anti-cleaved caspase-3 antibody (ab32042) were purchased from Abcam (Waltham, MA, USA). Anti-β-actin antibody (K101527P) was purchased from Solarbio Science & Technology Co., Ltd. (Beijing, China). Horseradish peroxidase (HRP) conjugated goat anti-mouse antibody (LF101) and HRP conjugated goat anti-rabbit antibody (LF102) were purchased from Epizyme Biotech Co., Ltd. (Shanghai, China).

2.2 Cell Culture

Human lung cancer A549 and H1299 cells were purchased from Procell Biotechnology (Wuhan, China) and cultured in DMEM supplemented with 10% FBS and 1% Penicillin-Streptomycin, under an atmosphere of 5% CO_2 at 37 °C. All cell lines were validated by STR profiling and tested negative for mycoplasma.

2.3 Isolation and Characterization of Turmeric-Derived Exosome-Like Nanoparticles

TELNs were isolated through multiple centrifugation steps and density gradient centrifugation as described earlier [14]. Fresh turmeric was washed three times with distilled water. The roots were then crushed in a juicer. Subsequently, the mixture was centrifuged at 1000 g for 10 minutes, followed by 3000 g for 20 minutes, and finally at 10,000 g for 30 minutes to collect the supernatant. The supernatant was filtered through a sterile 0.45 µm filter and placed in a fixed-angle rotor for centrifugation at 100,000 g for 1 h. The pellet was resuspended in 1 mL of PBS and subjected to sucrose gradient centrifugation at different concentrations (15%, 30%, 45%, and 60%) at a speed of 150,000 g for 2 h. The layer at the sucrose concentration of 30%–45% was collected, and an equal volume of PBS was added to wash away the sucrose. Finally, the mixture underwent centrifugation at 150,000 g for 1 h to collect the pellet, which was then resuspended in PBS as TELNs. The protein concentration of TELNs was measured with the bicinchoninic acid (BCA) assay. To verify that TELNs were successfully isolated, their structure was observed by transmission electron microscopy (TEM). Using a capillary pipette, one drop of the prepared suspension sample (5 µL of TELNs) was placed onto a copper grid coated with a support film. Excess liquid was absorbed with filter paper. Subsequently, a 3% phosphotungstic acid solution was added, and staining took place for 5 min. The staining solution was removed by filter paper, the sample was dried, and the morphology of TELNs was then examined and photographed by TEM (Jeol1230, JEOL Ltd., Peabody, MA, USA). The particle size distribution of TELNs was characterized by nanoparticle tracking analysis (NTA, PMX 110, ZetaView, Inning am Ammersee, Germany). Dynamic light scattering (DLS, ZS90, Malvern Panalytical Ltd., Worcestershire, UK) was utilized to measure the ζ-potential of TELNs. To determine curcumin in TELNs, TELNs were added to 1 mL of acetonitrile and sonicated to disrupt membranes, followed by centrifugation at 3000 rpm for 30 minutes. The supernatant was adjusted to a final volume of 2 mL with methanol and filtered through a 0.22 µm membrane to obtain the test solution. Curcumin was detected by Liquid Chromatography-Mass Spectrometry (LC-MS, 1290-6470A, Agilent Technologies, Inc., Santa Clara, CA, USA): Mobile phase: 0.1% formic acid-acetonitrile (1:1, v/v), flow rate: 0.3 mL/min, column temperature: 40 °C.

2.4 Cellular Uptake of Turmeric-Derived Exosome-Like Nanoparticles

PKH26-labeled TELNs were first prepared [15]. Briefly, 2 µM PKH67 dye and 1 mL Diluent C were mixed as a working solution. TELNs (50 µg) were then incubated with the working solution for 20 min at room temperature, and the labeled-TELNs were ultracentrifuged (100,000 g, 2 h) to remove free PKH26 dye. Subsequently, A549 cells (1×10^5 cells per well) were treated with PKH26-TELNs for 1, 2, and 4 h at 37 °C. After incubation, cells were washed 3 times with PBS solution. For laser confocal microscopy, cells were fixed with 4% (w/v) paraformaldehyde solution for 30 min. DAPI was then used to stain the nucleus, and cells were photographed under a laser confocal scanning microscope (LSM 910, ZEISS Group, Oberkochen, Germany). For flow cytometry, cells were collected and fixed with paraformaldehyde solution (4%, w/v). The uptake rate of PKH26-TELNs was then analyzed by flow cytometry (CytoFLEX V0-B5-R3, Beckman Coulter Life Sciences, Indianapolis, IN, USA).

2.5 Cell Counting Kit-8 (CCK-8) Assay

The cytotoxicity of TELNs against A549 cells was analyzed by CCK-8 assay [15]. Specifically, A549 cells (5×10^3 cells per well) were treated with TELNs (0, 5, 10, 20, 50, 100, 200 µg/mL) for 24 h. Subsequently, a 10% dilution of CCK-8 solution was added to the cells, and the plate was incubated for 1 h. The absorbance was then measured at 450 nm to determine cell viability.

2.6 Annexin V/PI Staining

TELNs-induced apoptosis was assessed by Annexin V/PI staining [15]. Specifically, after incubation with TELNs (0, 10, 50, and 100 µg/mL) for 24 h, cells were stained with the kit for 15 min and then analyzed by flow cytometry. Annexin V^+/PI^- cells were considered to be early apoptotic cells, while Annexin V^+/PI^+ cells were considered late apoptotic cells.

2.7 JC-1 Staining

A549 cells were seeded into 6-well plates (2×10^5 cells per well). After incubation with TELNs (0, 10, 50, and 100 µg/mL) for 24 h, cells were stained with JC-1 solution for 20 min in an incubator [16]. The JC-1 solution was then discarded, and the cells were washed three times with PBS before assessment by flow cytometry.

2.8 In Vivo Evaluation of Turmeric-Derived Exosome-Like Nanoparticles

Female nude mice (6-week-old) with a BALB/c genetic background were obtained from Liaoning Changsheng Biotechnology Co., Ltd. All animal experiments were conducted according to the guidelines of the Experimental Animal Welfare Ethics Committee of Changchun University of Chinese Medicine (2025936). The mice underwent a one-week acclimatization period before the establishment of the A549 hormonal nude model. Mice were anesthetized with isoflurane (induction concentration 3%, maintenance concentration 1%). After confirmation of anesthesia, 200 µL of an A549 cell suspension (5×10^6 cells/mL) was administered subcutaneously into each mouse [17]. Tumor size was measured by vernier caliper, and the tumor volume was calculated according to the formula $V = L \times S^2 \times 0.52$, where V is the volume, L is the longest diameter, and S is the shortest diameter. Based on preliminary experimental results, it was determined that each group required at least 5 animals. When the tumor volume reached 150 mm^3, the animals were divided into 4 groups of 5 mice each: PBS (control), TELNs 100 µg, TELNs 250 µg, and TELNs 500 µg. The groups underwent intratumoral injections every three days for a total of five times with 100 µL PBS, 100 µg TELNs, 250 µg TELNs, and 500 µg TELNs, respectively. Body weights and tumor volumes were recorded every three days. At day 18, mice were placed in an anesthesia chamber and perfused with CO_2 (flow rate 5 L/min) for euthanization. After confirming immobility, absence of respiration, and dilated pupils, the delivery of CO_2 was ceased. Mice were observed for 2 minutes to confirm death. Finally, tumor tissues were removed and evaluated using H&E staining.

2.9 RNA Extraction and Quantitative Real-Time Polymerase Chain Reaction (PCR)

A SteadyPure Universal RNA extraction kit (AG21017, ACCURATE BIOTECHNOLOGY, Changsha) was used to obtain total RNA from the tumor and A549 cells. All-in-One cDNA Synthesis SuperMix (TransGen Biotech Co., Ltd., Beijing, China) was used for reverse transcription. The quantitative real-time PCR mixture was formed with SYBR Green qPCR Master Mix for the Real-Time PCR System (QuantStudio 3, Thermo Fisher Scientific, Waltham, MA, USA). Relative changes in histone acetyltransferase human males absent on the first (hMOF) and GAPDH (Glyceraldehyde-3-Phosphate Dehydrogenase) mRNA levels were then measured. The primers [18] are shown in Table 1.

Table 1. Primer sequences for Real-time PCR.

Primer name	Sequence
hMOF forward	5′-GCTGGACGAGTGGGTAGACAA-3′
hMOF reverse	5′-TGGTGATCGCCTCATGCTCCTT-3′
GAPDH forward	5′-ATCACTGCCACCCAGAAGAC-3′
GAPDH reverse	5′-ATGAGGTCCACCACCCTGTT-3′

PCR, Polymerase Chain Reaction; hMOF, human males absent on first; GAPDH, Glyceraldehyde-3-Phosphate Dehydrogenase.

2.10 RNA Interference

A549 cells were transfected with siRNA oligonucleotides using Lipofectamine 2000 (Thermo Fisher Scientific, Waltham, MA, USA). The hMOF siRNA (5′-GAAAGAGAUCUACCGCAATT-3′) [19], Alexa Fluor 488 modified negative control siRNA (Cat no. 1027292), and unmodified negative control siRNA (Cat no. 1027280) were obtained from QIAGEN (USA). After transfection with siRNA, the cells were harvested for further analysis.

2.11 Wound Healing Assay

A549 cells were cultured in 6-well plates at a density of 5×10^5 cells per well. When cells reached 100% confluence, the monolayers in each well were scraped with a 200 µL pipette tip and washed three times with PBS. The cells were then followed with different treatments. Images were captured using an inverted microscope (IXplore, Olympus, Hachioji-shi, Tokyo, Japan) at 0, 12, 24, and 48 hours. Wound area was measured using ImageJ Fiji (National Institutes of Health, Washington, DC, USA) to calculate cell migration rates.

2.12 Curcumin-Non-Small Cell Lung Cancer Interaction Target Screening

(I) Curcumin target search. (i) Single-drug search: the SMILES chemical formula for the active ingredient of curcumin (CID: 969516) was obtained from the PubChem database (https://pubchem.ncbi.nlm.nih.gov/). The results were imported into the Swiss Target Prediction database (https://www.swisstargetprediction.ch/) to identify the target, and the target name was converted to gene name in the UniProt protein database (https://www.uniprot.org/). (ii) Herbal search: the target (sequence number: MOL000090) was retrieved from the TCMSP online database (https://www.tcmsp-e.com/), using curcumin as the keyword in the Chemical name entry. Its structure file was downloaded and imported into the PharmMapper database (https://www.lilab-ecust.cn/pharmmapper/) to retrieve the target moiety (Job ID: 250112151602). Target names were then converted to gene names in the UniProt protein database (https://www.uniprot.org/). The results from (i) and (ii) were combined to obtain the curcumin targets. (II) Target search in NSCLC. Using "non-small cell lung cancer" as the keyword, NSCLC-related targets were identified in the GeneCards (https://www.genecards.org/), OMIM (https://omim.org/), and Disgenet (https://disgenet.com) databases. The results were combined to remove duplicates and identify the targets. Finally, the intersecting targets for curcumin (I) and NSCLC (II) were determined.

2.13 Construction of the Protein-Protein Interaction (PPI) Network

The intersecting targets were imported into the STRING protein interactions database (http://string-db.org/), with the species set to homo sapiens and the Interaction score set to 0.400. The interaction proteins were screened, and the PPI network was constructed, with the results visualized using Cytoscape 3.10.3 software.

2.14 Gene Ontology and Kyoto Encyclopedia of Genes and Genomes Enrichment Analysis

(I) Intersecting target proteins were mapped to each term of the Gene Ontology (GO) database (http://www.geneontology.org/), and the protein number in each term was determined. GO terms that satisfied a p-value < 0.05 were selected as terms that were enriched in differential proteins. The function of these proteins was analyzed in three sections: cellular components, molecular function, and biological processes.

(II) The intersecting targets were mapped to pathways using the Kyoto Encyclopedia of Genes and Genomes (KEGG) database (https://www.genome.jp/kegg/). Significantly enriched KEGG pathways were identified as having a p-value < 0.05.

2.15 Molecular Docking

Curcumin and hMOF protein were selected for molecular docking analysis. The 3D structure for the active ingredient of curcumin (CID: 969516) was obtained from the PubChem database (https://pubchem.ncbi.nlm.nih.gov/). and that of hMOF protein (ID: pdb_00004dnc) from the PDB database (http://www.rcsb.org/). Water and ligand were removed from the receptor with PyMOL 3.1 (Schrödinger Inc., New York City, NY, USA), then converted to pdbqt format using Auto Dock 4.2.6 (Scripps Research Institute, Claremont, CA, USA). Appropriate positions were selected for docking. Binding energies were calculated and the results were visualized using PyMOL 3.1 (Schrödinger Inc., New York City, NY, USA).

2.16 Western Blot Assay

Cells were lysed using RIPA lysis buffer (89900, Thermo Fisher Scientific, Waltham, MA, USA) containing a 1% protease inhibitor mixture (87785, Thermo Fisher Scientific, Waltham, MA, USA). The protein concentration was subsequently determined using a BCA protein assay kit (P0012, Beyotime Biotechnology Co., Ltd., Shanghai, China). Protein samples were separated by 10% sodium dodecyl sulfate polyacrylamide gel electrophores (SDS-PAGE) gel electrophoresis (XP00100BOX, Thermo Fisher Scientific, Waltham, MA, USA) and transferred to polyvinylidene fluoride (PVDF) membranes (Millipore). The membrane was then blocked for 1 h in Tris-buffered saline (TBS) containing 5% skim milk at room temperature, followed by overnight incubation at 4 °C with the primary antibody: Anti-hMOF antibody (1:1000; ab200660, Abcam), anti-H4K16ac antibody (1:1000; ab109463, Abcam), anti-histone H4 antibody (1:1000; ab7311, Abcam), anti-procaspase-3 antibody (1:1000; ab32150, Abcam), anti-cleaved caspase-3 antibody (1:1000; ab32042, Abcam), anti-β-actin antibody (1:1000; K101527P, Solarbio). After three washes, the membrane was incubated at room temperature for 45 minutes with horseradish peroxidase (HRP)-labeled secondary antibody: HRP conjugated goat anti-mouse antibody (1:1000; LF101, Epizyme Biotech), HRP conjugated goat anti-rabbit antibody (1:1000; LF102, Epizyme Biotech). The PVDF membrane was developed with a chemiluminescence detection analysis system (iBright CL750, Thermo Fisher Scientific, Waltham, MA, USA), and the images were then analyzed using ImageJ software.

2.17 Statistical Analysis

Results are presented as the mean $\pm$ SD. To ensure the reproducibility of results, experiments were repeated three times. Differences were analyzed using one-way ANOVA with Tukey's multiple comparisons test. p-values < 0.05 were considered statistically significant, with $p < 0.01$ and $p < 0.001$ indicating highly and extremely significant differences, respectively.

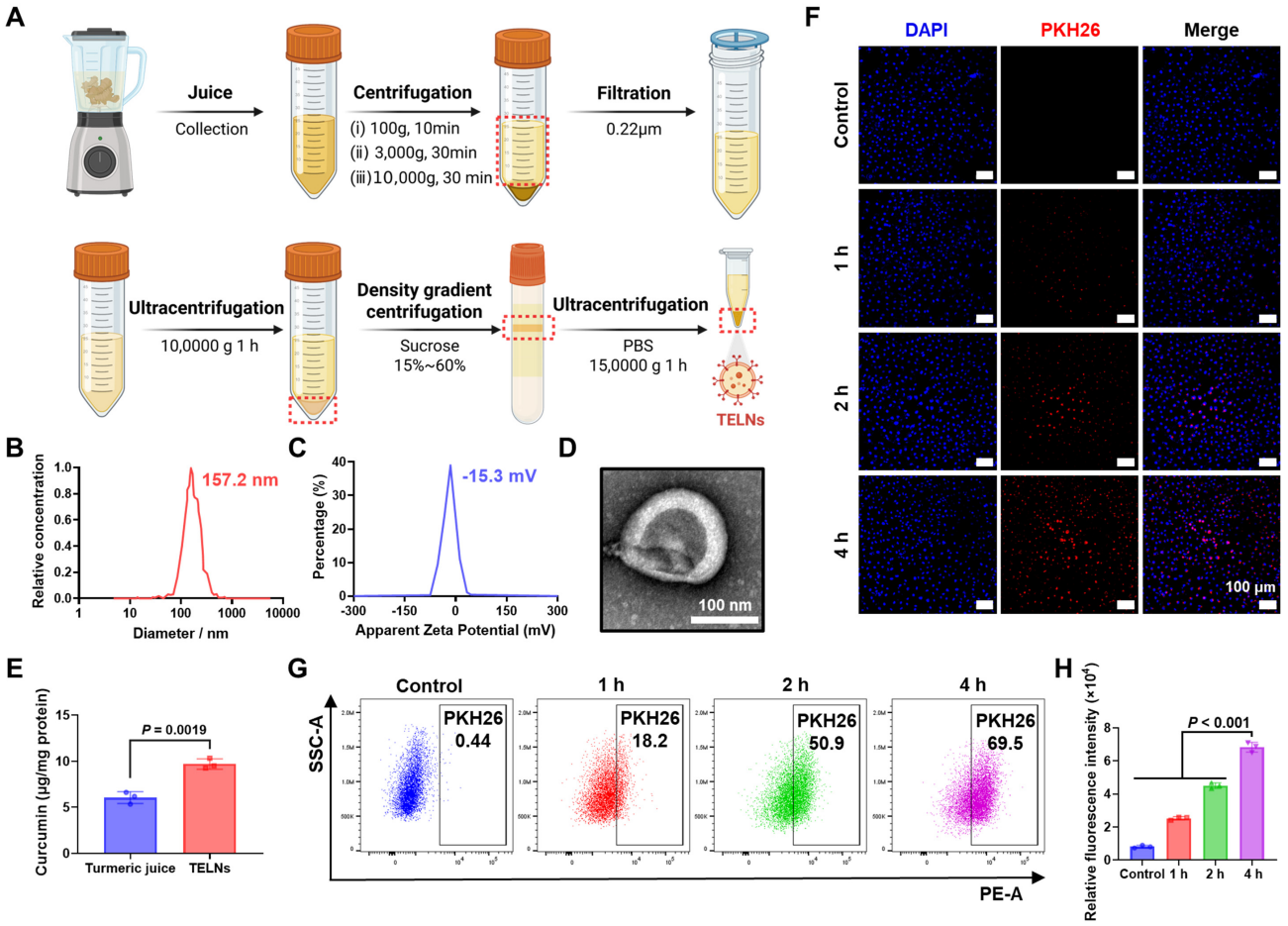

Fig. 1. Extraction, characterization, and uptake analysis of turmeric-derived exosome-like nanoparticles. (A) Procedure for extracting TELNs. (B) Nanoparticle tracking analysis (NTA) of TELNs, showing a particle size of 157.2 nm. (C) Zeta potential analysis of TELNs, indicating a ζ-potential of –15.3 mV. (D) Transmission electron microscopy (TEM) image of TELN, scale bar: 100 nm. (E) Detection of curcumin in TELNs by Liquid Chromatography-Mass Spectrometry. (F) Cellular uptake of TELNs by A549 cells after 1, 2, and 4 h, as detected by laser scanning confocal microscopy (red: PKH26-labelled TELNs; blue: nuclei staining; scale bar: 100 μm). (G) Cellular uptake of TELNs by A549 cells at 1, 2, and 4 h, as measured by flow cytometry. (H) Quantitative analysis by flow cytometry (n = 3). TELNs, turmeric-derived exosome-like nanoparticles; DAPI, 4′,6-diamidino-2-phenylindole.

3. Results

3.1 Extraction, Characterization, and Uptake Analysis of Turmeric-Derived Exosome-Like Nanoparticles

To obtain TELNs, turmeric was juiced and then subjected to differential centrifugations and density gradient centrifugation (Fig. 1A). The physical properties of the TELNs were subsequently characterized. The size distribution of TELNs was measured using nanoparticle tracking analysis (NTA). TELNs showed a particle size of 157.2 nm (Fig. 1B), and their ζ-potential was –15.3 mV (Fig. 1C). TEM revealed that TELNs exhibited an exosome-like morphology, characterized by a bilayer membrane vesicle (Fig. 1D). TELNs demonstrated stability, with no significant change in diameter over a 7-day period (**Supplementary Fig. 1**). TELNs were found to be enriched with higher concentrations of curcumin compared to turmeric juice (Fig. 1E; **Supplementary Fig. 2**). The release profile of TELNs indicated that 79.93% of curcumin was released within 24 hours (**Supplementary Fig. 3**). The above results demonstrate the successful isolation of TELNs from plant tissue. To evaluate the cellular uptake efficiency, PKH26-labeled TELNs were incubated with A549 cells. Confocal laser scanning microscopy images revealed that TELNs were taken up by A549 cells, with a significant effect observed at 4 h (Fig. 1F; **Supplementary Fig. 4**). Quantitative flow cytometry results also supported this conclusion. At 4 h, 69.5% of cells were positive, demonstrating that TELNs could effectively enter A549 cells (Fig. 1G,H). In summary, TELNs were successfully isolated from turmeric. Moreover, they exhibit exosome-like characteristics and can be internalized by NSCLC cells.

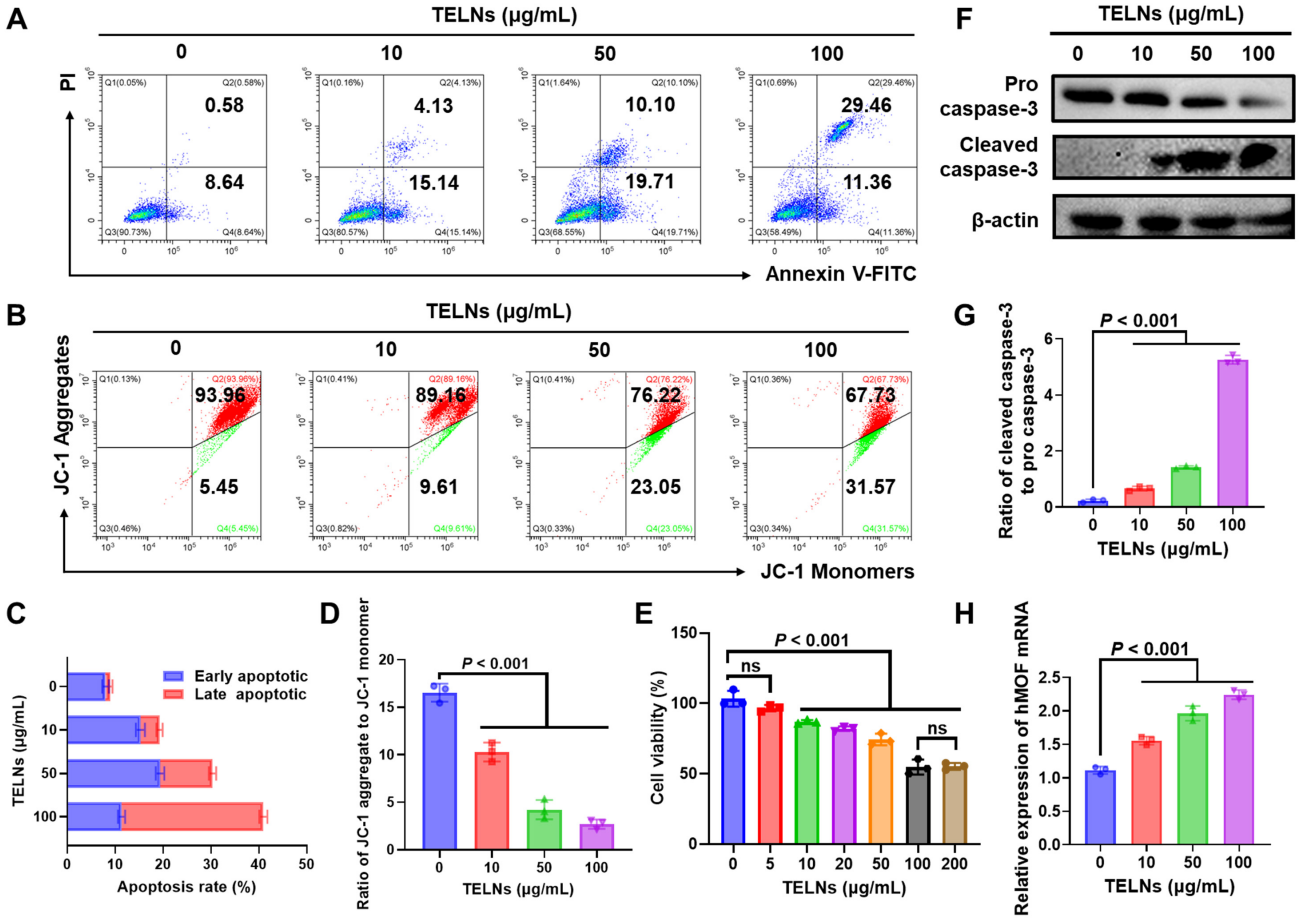

Fig. 2. Turmeric-derived exosome-like nanoparticles induce apoptosis in non-small cell lung cancer. (A) Apoptosis of TELN-treated A549 cells, as measured by flow cytometry. (B) Mitochondrial membrane potential of A549 cells, as detected by flow cytometry. (C) Apoptosis rate of A549 cells (n = 3). (D) Ratio of JC-1 aggregate to JC-1 monomer (n = 3). (E) Cytotoxicity of TELNs against A549 cells, as measured by CCK-8 assay (n = 3), ns indicates that the results are not significant. (F) Western blot analysis of pro and cleaved caspase-3 expression in A549 cells after treatment. (G) The ratio of cleaved caspase-3 to pro caspase-3 (n = 3). (H) hMOF mRNA levels analyzed by real-time PCR (n = 3). JC-1, 5,5,6,6′-tetrachloro-1,1′,3,3′ tetraethylbenzimi-dazoylcarbocyanine iodide; CCK-8, Cell Counting Kit-8; hMOF, human males absent on first; PCR, Polymerase Chain Reaction.

3.2 Turmeric-Derived Exosome-Like Nanoparticles Induce Apoptosis in Non-Small Cell Lung Cancer

We first assessed the effect of TELNs on apoptosis in NSCLC. Flow cytometry analysis revealed the apoptosis rate of A549 cells treated with 100 μg/mL TELNs was 4.54–fold higher compared to the control group, with late-stage apoptosis increasing from 1.02% to 29.60% (Fig. 2A,C). Additionally, 100 μg/mL TELNs increased the apoptosis rate of H1299 cells by 45.46% (**Supplementary Fig. 5**). Consistent with these observations, CCK-8 assays revealed dose-dependent anti-NSCLC activity of TELNs, with a 45.25% reduction in cell viability at 100 μg/mL (Fig. 2E). The same phenomenon was also observed in H1299 cells, where TELNs demonstrated anticancer activity. At a dose of 100 μg/mL, the viability of H1299 cells decreased by 44.67% (**Supplementary Fig. 6**). The JC-1 probe is commonly used to detect the membrane potential of mitochondria, which is closely related to apoptosis. When apoptosis occurs, the mitochondrial membrane is destroyed, and JC-1 changes from an aggregated state to a dispersed state. Thus, enhanced green fluorescence (JC-1 monomers) implies increased apoptosis. TELNs significantly induced mitochondria-related apoptosis in A549 cells (Fig. 2B,D). The expression of cleaved caspase-3 protein was examined by Western blot assay to corroborate the presence of apoptosis. As a crucial executor of apoptosis, caspase-3 translocates from the mitochondria and induces apoptosis. TELNs significantly increased the ratio of cleaved caspase-3 to pro caspase-3 in A549 cells (Fig. 2F,G). Similarly, TELNs also increased the ratio in H1299 cells (**Supplementary Fig. 7**). Additionally, real-time quantitative PCR revealed that hMOF mRNA expression increased 2.01–fold in A549 cells (Fig. 2H) and 1.82–fold in H1299 cells (**Supplementary Fig. 8**) following treatment with TELNs. Collectively, these findings establish TELNs as inducers of apoptosis in A549 cells, with hMOF being a critical factor.

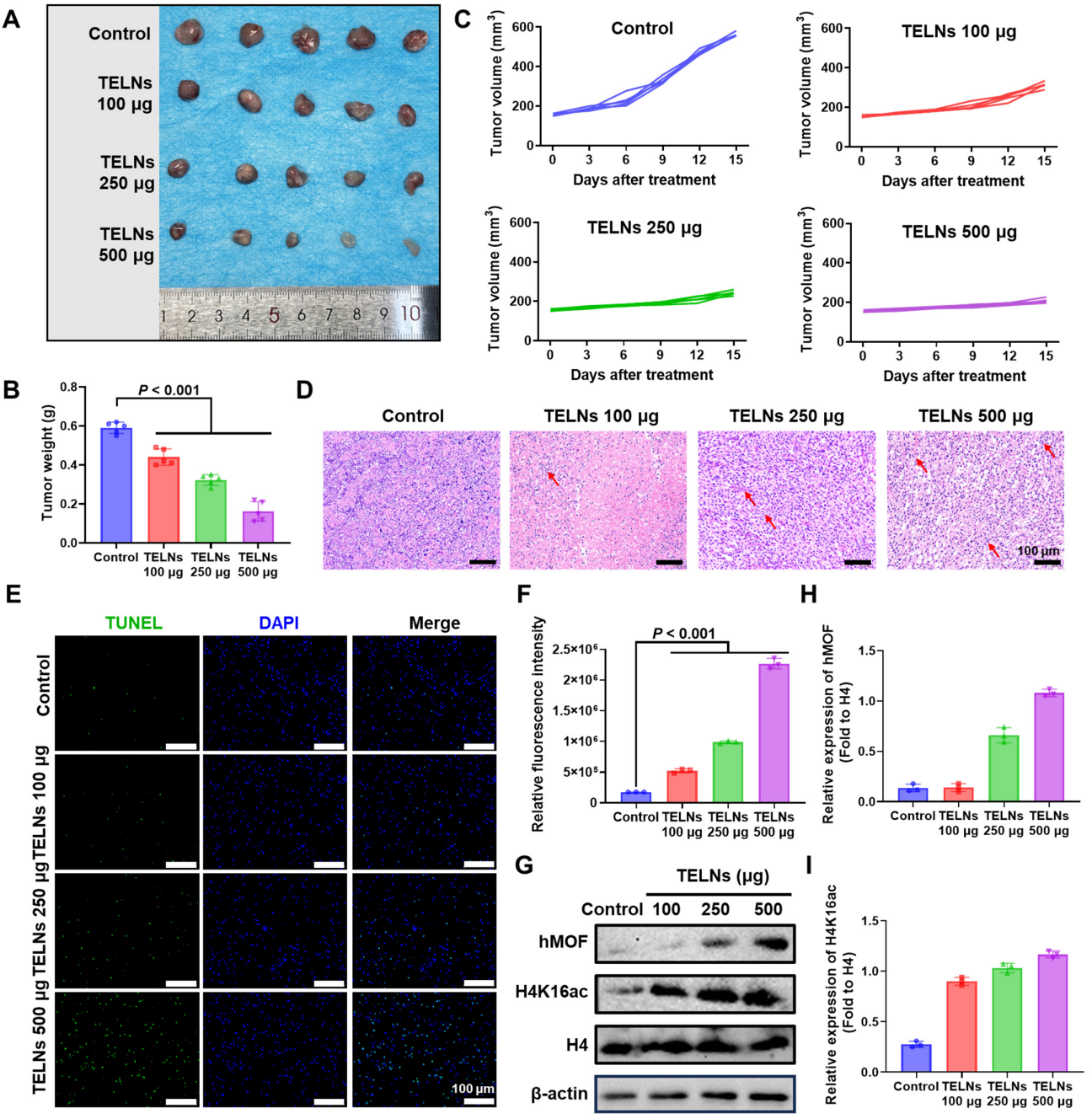

Fig. 3. Turmeric-derived exosome-like nanoparticles inhibit non-small cell lung cancer progression *in vivo*. (A) Images of tumors from mice after treatment with TELNs (n = 5). (B) Tumor weight after treatment (n = 5). (C) Changes in tumor volume over time (n = 5). (D) H&E staining images of tumor tissue (scale bar: 100 μm; red arrows indicate the cellular disorganization). (E) TUNEL staining of tumor (green: TUNEL; blue: nuclei staining; scale bar: 100 μm). (F) Quantitative analysis of fluorescence intensity (n = 3). (G) hMOF and H4K16ac levels in tumor detected by Western blot assay. (H) The expression of hMOF quantified by ImageJ software (n = 3). (I) The expression of H4K16ac quantified by ImageJ software (n = 3). TUNEL, Terminal deoxynucleotidyl transferase dUTP nick end labeling; H4K16ac, histone H4K16 acetylation.

3.3 Turmeric-Derived Exosome-Like Nanoparticles Inhibit Non-Small Cell Lung Cancer Progression In Vivo

An A549 xenograft nude mouse model was established to evaluate the antitumor efficacy of TELNs *in vivo*. Compared to the control group, treatment with TELNs resulted in a 58.1% reduction in tumor volume, confirming its potent growth-inhibitory effects (Fig. 3A,B). In tests conducted every three days, treatment with TELNs significantly slowed tumor growth (Fig. 3C). H&E staining of the tumor tissue revealed distinct morphological differences, with PBS-treated tumors displaying uniform cell

size, whereas TELN-treated tumors exhibited marked cellular disorganization (Fig. 3D). TUNEL staining showed a significant increase in apoptosis after treatment with TELNs (Fig. 3E,F). Since hMOF is known to catalyze histone H4K16 acetylation (H4K16ac), downstream epigenetic modulation was also examined.

Western blot analysis of tumor tissues revealed that TELNs significantly increased the levels of hMOF and H4K16ac (Fig. 3G–I). This suggested that hMOf and H4K16ac may serve as the target through which TELNs promote apoptosis in NSCLC. These findings demonstrate that TELNs effectively inhibited NSCLC progression and upregulated hMOF and H4K16ac *in vivo*.

3.4 Turmeric-Derived Exosome-Like Nanoparticles Inhibit Non-Small Cell Lung Cancer by Upregulating hMOF and Histone H4K16 Acetylation

Building upon previous studies examining the efficacy of TELNs in NSCLC, we conducted further investigations to determine whether its activity depends on the induction of hMOF. RNA interference was employed as a knockdown method, and the AF488-labeled Negative Control demonstrated an siRNA transfection efficiency of 80.4% for this approach (**Supplementary Fig. 9**). sihMOF effectively reduced hMOF expression by 86.22% (**Supplementary Fig. 10**). hMOF knockdown substantially reduced JC-1 monomer formation, suggesting impaired apoptosis. Notably, treatment with TELNs partially rescued this effect, demonstrating the role of TELNs in hMOF regulation (Fig. 4A,B). Consistent with the above observations, direct assessment of apoptosis rates revealed that silencing of hMOF decreased cell death by 54.28%, while treatment with TELNs restored apoptosis by 13.13% (Fig. 4C,D). Furthermore, wound healing assays were performed to analyze the effect of TELNs on cell migration. Scratch closure rates were quantified at 12, 24, and 48 h. Knockdown of hMOF enhanced A549 cell migration by 31.70% in 48 h, whereas TELNs partially counteracted the pro-migration effects induced by hMOF downregulation (Fig. 4E,F). These findings indicate that TELNs inhibit NSCLC cell migration by upregulating hMOF expression. Western blot assay further demonstrated suppression of both hMOF and H4K16ac expression after hMOF knockdown. Crucially, TELNs restored H4K16ac levels, consistent with their ability to upregulate hMOF (Fig. 4G–I). Collectively, these data establish the hMOF-H4K16ac axis as a key pathway through which TELNs exert their suppressive effects on NSCLC.

3.5 Epigenetic Regulation of Turmeric-Derived Exosome-Like Nanoparticles is Associated With Curcumin

As expected, TELNs possess multiple properties of turmeric. In a previous study, Wei *et al*. [20] demonstrated that TELNs contain a high concentration of curcumin. Curcumin is a natural compound extracted from turmeric that exhibits anticancer properties through its impact on epigenetic modifications [21,22]. However, its regulatory role in hMOF remains unclear. Therefore, we hypothesized that epigenetic regulation by TELNs is related to the curcumin contained within them. We conducted a systematic bioinformatics analysis to elucidate the molecular mechanism underlying this effect. First, the chemical structure of curcumin (Fig. 5A) was used to search for interacting proteins, which were then compared with NSCLC-related proteins. The database identified 324 curcumin target proteins and 3782 NSCLC-associated proteins, with 191 overlapping targets highlighted by a Venn map (Fig. 5B). The protein-protein interaction (PPI) network was performed using the STRING database (**Supplementary Fig. 11**), with parameters set to Homo sapiens and the interaction score at 0.400. The network comprised 191 nodes and 920 edges, with an average node degree of 9.63, indicating extensive connections among the proteins. KEGG pathway enrichment analysis revealed these proteins were highly associated with cancer progression, VEGF signaling, PD-L1 immune checkpoint regulation, and the development of NSCLC (**Supplementary Fig. 12**). Furthermore, GO enrichment analysis (Fig. 5C–E) categorized the overlapping proteins into three functional subsets: (i) cellular component (CC): localized in the cytoplasm and nucleus; (ii) biological process (BP): involved in histone remodeling, apoptosis, and response to reactive oxygen species (ROS); (iii) molecular function (MF): enriched in DNA binding, histone H4K16 acetylation, and protease activity. The overlapping targets were visualized using Cytoscape software. This revealed significant enrichment of KAT8, KAT6A, KAT6B, KAT5, and KAT7 (all members of the hMOF histone acetyltransferase family), suggesting the anti-tumor activity of curcumin was closely linked to the regulation of histone H4K16 acetylation (Fig. 5F). We next investigated whether curcumin directly interacts with hMOF to modulate its function. Molecular docking analysis was performed using PDB software to simulate the binding between curcumin and KAT8. The calculated binding energy of –6.7 kcal/mol (significantly below the threshold of –5 kcal/mol) strongly supports a stable interaction between curcumin and hMOF (Fig. 5G). Collectively, these results demonstrate that curcumin in TELNs upregulates hMOF expression and H4K16ac in A549 cells. Mechanistically, molecular docking suggested curcumin may interact with hMOF. In brief, curcumin in TELNs promotes H4K16 acetylation by activating hMOF, thereby promoting apoptosis and inhibiting NSCLC. This reveals a new epigenetic regulatory mechanism.

4. Discussion

This study successfully isolated TELNs and validated their anti-cancer efficacy both *in vitro* and *in vivo*. Moreover, a novel epigenetic mechanism was elucidated in which TELNs inhibit NSCLC through hMOF. Bioinformat-

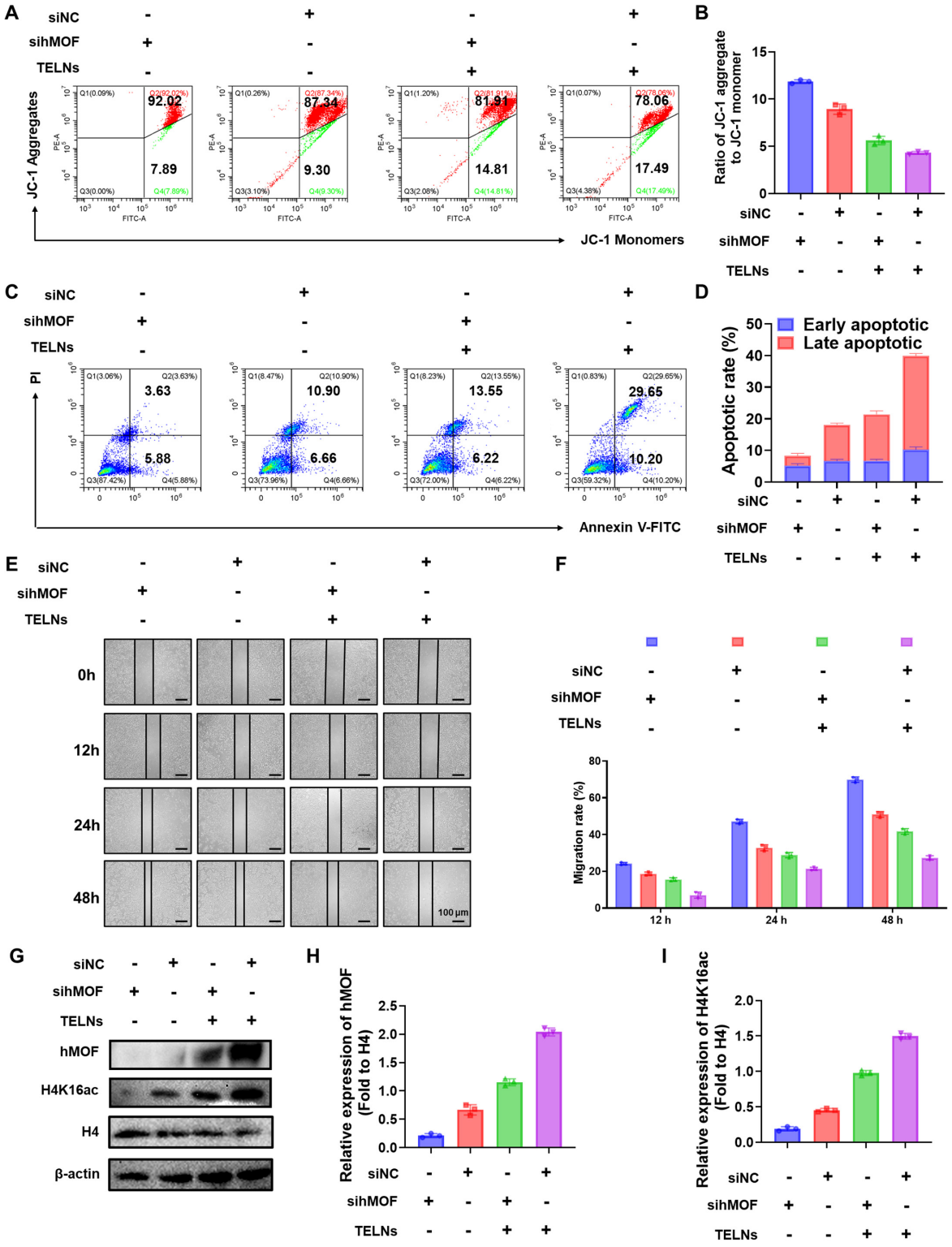

Fig. 4. Turmeric-derived exosome-like nanoparticles inhibit non-small cell lung cancer by upregulating hMOF expression and histone H4K16 acetylation. (A) Mitochondrial membrane potential of A549 cells, as detected by flow cytometry. (B) Ratio of JC-1 aggregate to JC-1 monomer (n = 3). (C) Apoptosis of A549 cells, as measured by flow cytometry. (D) Early and late apoptosis rates of different groups (n = 3). (E) Wound healing assay for A549 cells observed under a microscope at 12 h, 24 h, and 48 h (scale bar: 200 μm). (F) Analysis of cell migration rate (n = 3). (G) Effect of TELNs on hMOF and H4K16ac levels in A549 cells, as detected by Western blot. (H) The expression of hMOF quantified by ImageJ software (n = 3). (I) The expression of H4K16ac quantified by ImageJ software (n = 3). "+"/ "-" indicate whether cells were treated with siRNA or TELNs. siNC, Negative Control siRNA; sihMOF, hMOF siRNA; FITC, Fluorescein isothiocyanate; H4, Histone H4.

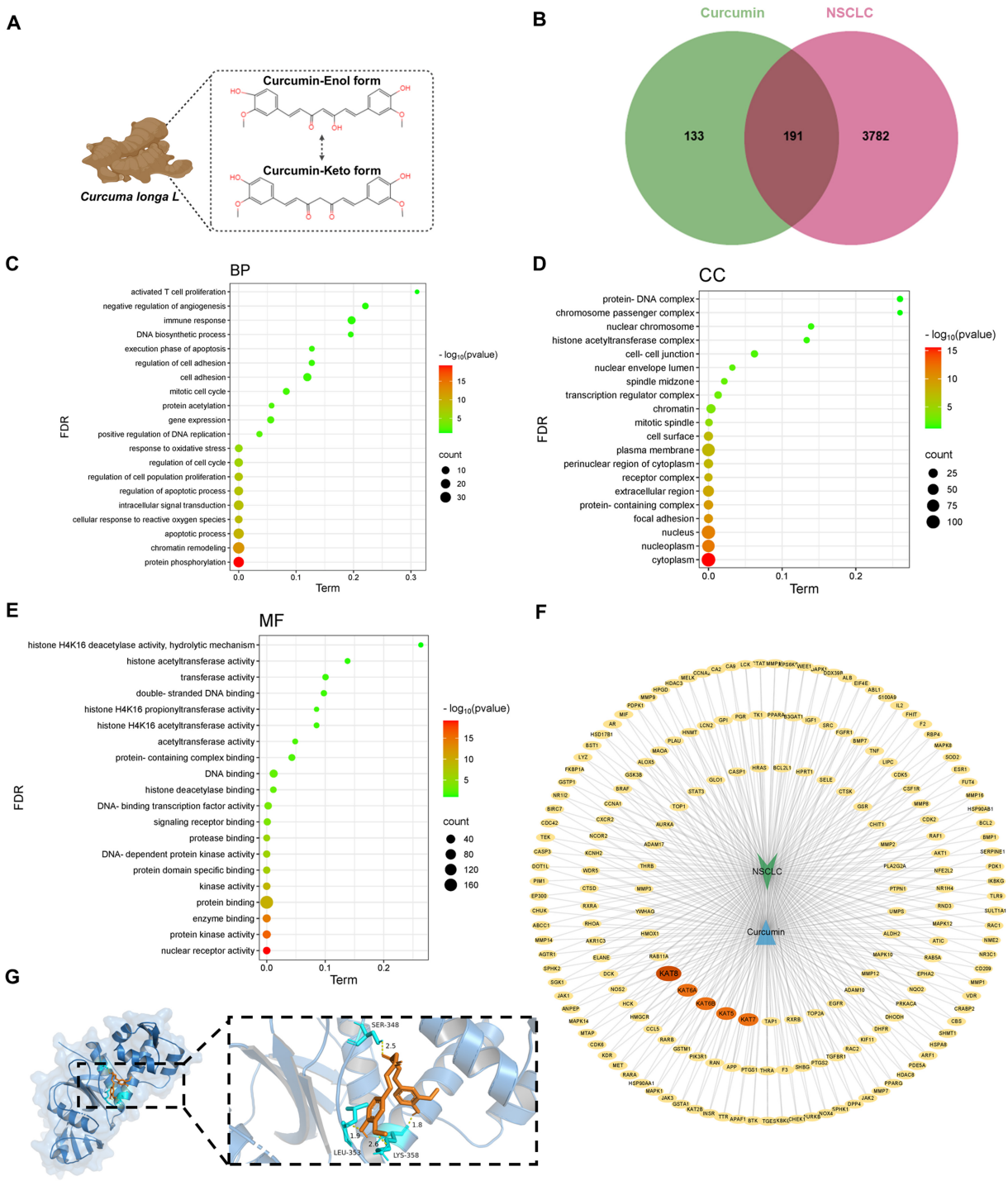

Fig. 5. Epigenetic regulation by turmeric-derived exosome-like nanoparticles is due to curcumin. (A) Chemical structure of curcumin. (B) Venn map showing the intersection of curcumin and NSCLC targets. (C) GO enrichment analysis: biological process. (D) GO enrichment analysis: cellular component. (E) GO enrichment analysis: molecular function. (F) "Curcumin-NSCLC" target protein network. (G) Molecular docking simulation of curcumin with hMOF. BP, biological process; CC, cellular component; MF, molecular function; FDR, False Discovery Rate; NSCLC, non-small cell lung cancer.

ics and experimental analyses identified hMOF as a pivotal target, with curcumin in TELNs enhancing the levels of both hMOF and histone H4 at lysine 16 (H4K16ac) (Fig. 6).

Plant-derived exosome-like nanoparticles (PELNs) are nanoscale vesicles secreted by plants and exhibit bioactivity and biocompatibility [23]. PELNs carry lipids, proteins, miRNAs, and other components, exhibiting a similar structure to mammalian exosomes. They also offer advantages such as large-scale production capacity and natural therapeutic components [24]. Researchers have highlighted

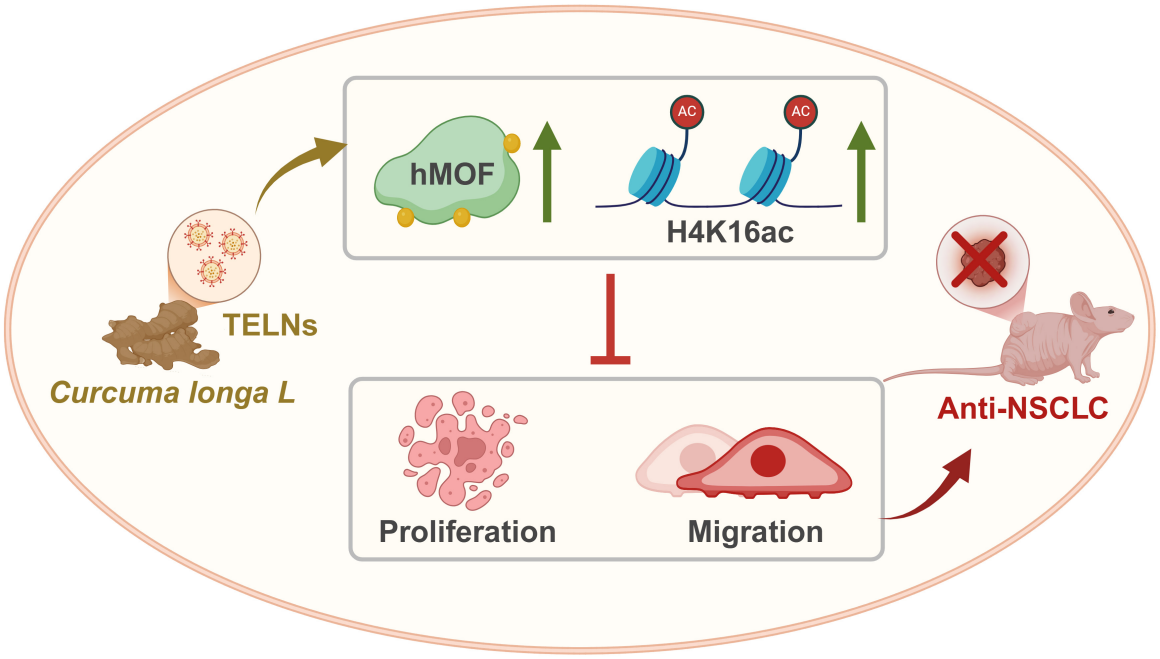

Fig. 6. Mechanism underlying the anti-cancer effect of turmeric-derived exosome-like nanoparticles. TELNs upregulate hMOF and histone H4K16 acetylation, thereby promoting apoptosis and inhibiting NSCLC. The green upward arrow indicates increased expression.

the anticancer effects of PELNs, including ginger-derived nanoparticles (GDENs) that induce apoptosis in cancer through TRAIL-mediated processes [25], and grapefruit-derived vesicles that deliver chemotherapeutics to tumor sites [26]. However, the epigenetic regulatory mechanisms of PELNs have not been studied. Our study bridges this gap by isolating turmeric-derived exosome-like nanoparticles (TELNs) and investigating the epigenetic mechanism underlying their anti-NSCLC effects. Originally defined as the interaction between genotype and phenotype, epigenetics primarily involves chromatin structural modifications that regulate gene expression [27]. Epigenetic research has provided insights into NSCLC progression and the mechanisms underlying anti-NSCLC drugs [28]. Histone acetylation, a pivotal epigenetic modification, adds an acetyl group to lysine residues on histones. This process is regulated by both histone acetyltransferases (HATs) and histone deacetylases (HDACs), which maintain acetylation homeostasis [29]. MOF is a MYST family member of HATs and specifically acetylates histone H4 at lysine 16 (H4K16ac) [30]. Notably, the expression of hMOF differs significantly between NSCLC and normal tissues [31]. By modulating the H4K16ac modification, hMOF promotes transcriptional activation and DNA repair, thereby regulating NSCLC progression [32]. TELNs significantly inhibit NSCLC progression *in vitro* and *in vivo*. Treatment with 100 μg/mL of TELNs induced apoptosis in A549 and H1299 cells and reduced tumor volume by 58.1%. These effects were mediated through upregulation of the histone acetyltransferase hMOF and its product H4K16ac. Molecular docking suggested potential interaction of curcumin to hMOF, while hMOF knockdown experiments confirmed the effects of TELNs. This dual action—upregulating both the expression and activity of hMOF—makes TELNs a unique epigenetic regulator.

Curcumin is a natural polyphenol isolated from the rhizome of *Curcuma longa* [33]. Accumulating evidence has demonstrated multiple mechanisms by which curcumin inhibits NSCLC progression [34], including downregulation of cyclin expression, induction of A549 cell cycle arrest, and suppression of cell proliferation [35]. Additionally, it promotes apoptosis in multiple pathways [36]. Although curcumin demonstrates anticancer effects against NSCLC, its poor bioavailability and low water solubility significantly hinder its translational application [37]. However, TELNs can overcome the bioavailability limitations of curcumin, with their phospholipid bilayer protecting cargoes from degradation. The particle size of TELNs in the present study remained stable during testing. Moreover, TELNs have dual functions as drug carriers and epigenetic modulators. As plant-derived nanoparticles, TELNs not only exhibit anticancer effects, but also serve as drug delivery systems capable of carrying various medications. Liposomes loaded with curcumin (CURLipo) have been developed (via ethanol injection method) for comparison with TELNs [38]. CUPLipo exhibits similar properties to TELNs with regard to uptake efficiency by A549 cells (Fig. 1G,H; **Supplementary Fig. 13**) and stability (**Supplementary Figs. 1**,**14**). However, TELNs demonstrated superior anti-NSCLC efficacy (**Supplementary Fig. 15**). Furthermore, hemolysis assays revealed that TELNs exhibited superior safety compared to

CURLipo (**Supplementary Fig. 16**). This indicates that TELNs, as natural curcumin delivery carriers, offer advantages over liposomes.

The present study demonstrates for the first time that TELNs suppress NSCLC by epigenetic regulation. TELNs overcome the bioavailability limitations of curcumin, thus serving as a natural nanotherapeutic platform. However, their clinical translation requires further evaluation in more complex tumor models. Additionally, as TELNs are natural products derived from turmeric, standardized protocols must be established to overcome batch-to-batch variability in translational applications.

5. Conclusion

This study explored the anti-cancer mechanism of turmeric-derived exosome-like nanoparticles (TELNs). TELNs were found to regulate the histone acetyltransferase hMOF and histone H4 at lysine 16 (H4K16ac). They significantly induced apoptosis in non-small cell lung cancer (NSCLC), upregulated hMOF expression, and enhanced H4K16 acetylation. These findings establish for the first time that TELNs exert anti-tumor effects through epigenetic regulation of hMOF/H4K16ac, thus providing a basis for plant-derived nanoparticle-based therapies in cancer treatment.

Availability of Data and Materials

The datasets used in this article are accessible from the corresponding author DL upon request.

Author Contributions

Conceptualization: WS; Methodology: WS, DL; Software: WS; Validation: WS, DL, ZZ; Formal Analysis: WS; Investigation: WS; Data Curation: DL; Writing–Original Draft: WS; Writing–Review & Editing: DL, ZZ; Visualization: WS; Supervision: DL, ZZ; Project Administration: DL, ZZ; Funding Acquisition: DL, ZZ; Resources: ZZ. All authors contributed to editorial changes in the manuscript. All authors read and approved the final manuscript. All authors have participated sufficiently in the work and agreed to be accountable for all aspects of the work.

Ethics Approval and Consent to Participate

The experimental procedures involving animals were conducted according to the Experimental Animal Welfare Ethics Committee of Changchun University of Chinese Medicine (Approval number: 2025936), Jilin Province, China.

Acknowledgment

We acknowledged the support of Biorender, Fig. 1A and Fig. 6 were created in https://biorender.com.

Funding

The authors declare this study was funded by a grant from National Natural Science of China (No. 81803680) and a grant from Natural Science of Jilin Province (No. YDZJ202401082ZYTS).

Conflict of Interest

The authors declare no conflict of interest.

Supplementary Material

Supplementary material associated with this article can be found, in the online version, at https://doi.org/10.31083/FBL47950.

References

[1] Bray F, Laversanne M, Sung H, Ferlay J, Siegel RL, Soerjomataram I, *et al*. Global cancer statistics 2022: GLOBOCAN estimates of incidence and mortality worldwide for 36 cancers in 185 countries. CA: a Cancer Journal for Clinicians. 2024; 74: 229–263. https://doi.org/10.3322/caac.21834.

[2] Vaidya JS. Principles of cancer treatment by radiotherapy. Surgery (Oxford). 2024; 42: 139–149. https://doi.org/10.1016/j.mpsur.2023.12.001.

[3] Khazaei Monfared Y, Heidari P, Klempner SJ, Mahmood U, Parikh AR, Hong TS, *et al*. DNA Damage by Radiopharmaceuticals and Mechanisms of Cellular Repair. Pharmaceutics. 2023; 15: 2761. https://doi.org/10.3390/pharmaceutics15122761.

[4] Xi Z, Dai R, Ze Y, Jiang X, Liu M, Xu H. Traditional Chinese medicine in lung cancer treatment. Molecular Cancer. 2025; 24: 57. https://doi.org/10.1186/s12943-025-02245-6.

[5] Yi C, Lu L, Li Z, Guo Q, Ou L, Wang R, *et al*. Plant-derived exosome-like nanoparticles for microRNA delivery in cancer treatment. Drug Delivery and Translational Research. 2025; 15: 84–101. https://doi.org/10.1007/s13346-024-01621-x.

[6] Zhang F, Liang X, Liu H, Anayyat U, Yang Z, Wang X. Advancements and Challenges of Plant-derived Extracellular Vesicles in Anti-Cancer Strategies and Drug Delivery. Current Drug Delivery. 2025; 22: 921–934. https://doi.org/10.2174/0115672018367056250227074828.

[7] Kim J, Li S, Zhang S, Wang J. Plant-derived exosome-like nanoparticles and their therapeutic activities. Asian Journal of Pharmaceutical Sciences. 2022; 17: 53–69. https://doi.org/10.1016/j.ajps.2021.05.006.

[8] Zhao B, Lin H, Jiang X, Li W, Gao Y, Li M, *et al*. Exosome-like nanoparticles derived from fruits, vegetables, and herbs: innovative strategies of therapeutic and drug delivery. Theranostics. 2024; 14: 4598–4621. https://doi.org/10.7150/thno.97096.

[9] Nemati M, Singh B, Mir RA, Nemati M, Babaei A, Ahmadi M, *et al*. Plant-derived extracellular vesicles: a novel nanomedicine approach with advantages and challenges. Cell Communication and Signaling: CCS. 2022; 20: 69. https://doi.org/10.1186/s12964-022-00889-1.

[10] Tian WW, Liu L, Chen P, Yu DM, Li QM, Hua H, *et al*. Curcuma Longa (turmeric): from traditional applications to modern plant medicine research hotspots. Chinese Medicine. 2025; 20: 76. https://doi.org/10.1186/s13020-025-01115-z.

[11] Aziz MNM, Rahim NFC, Hussin Y, Yeap SK, Masarudin MJ, Mohamad NE, *et al*. Anti-Metastatic and Anti-Angiogenic Effects of Curcumin Analog DK1 on Human Osteosarcoma Cells In Vitro. Pharmaceuticals (Basel, Switzerland). 2021; 14: 532. https://doi.org/10.3390/ph14060532.

[12] Dytrych P, Kejík Z, Hajduch J, Kaplánek R, Veselá K,

Kučnirová K, *et al*. Therapeutic potential and limitations of curcumin as antimetastatic agent. Biomedicine & Pharmacotherapy. 2023; 163: 114758. https://doi.org/10.1016/j.biopha.2023.114758.

[13] Yang X, Peng Y, Wang Y-e, Zheng Y, He Y, Pan J, *et al*. Curcumae Rhizoma Exosomes-like nanoparticles loaded Astragalus components improve the absorption and enhance anti-tumor effect. Journal of Drug Delivery Science and Technology. 2023; 81: 104274. https://doi.org/10.1016/j.jddst.2023.104274.

[14] Liu C, Yan X, Zhang Y, Yang M, Ma Y, Zhang Y, *et al*. Oral administration of turmeric-derived exosome-like nanovesicles with anti-inflammatory and pro-resolving bioactions for murine colitis therapy. Journal of Nanobiotechnology. 2022; 20: 206. https://doi.org/10.1186/s12951-022-01421-w.

[15] Zhang H, Xing J, Sun M, Cui Y, Li Y, Hu S, *et al*. Engineered exosomes for targeted microRNA delivery to reverse liver fibrosis. Biomaterials. 2026; 324: 123510. https://doi.org/10.1016/j.biomaterials.2025.123510.

[16] Jin Y, Jia X, Fan D, Zhou X, Tan X, Liu D, *et al*. *Ganoderma lucidum* Glycoprotein Microemulsion: Improved Transdermal Delivery and Protective Efficacy in UV-Induced Cell and Animal Models. Molecules (Basel, Switzerland). 2025; 30: 4489. https://doi.org/10.3390/molecules30224489.

[17] Wang S, Jiang H, Liu J, Chen J, Hu S, Cui Y, *et al*. LPAR4-targeted dual-loaded liposome for synergistic lung cancer therapy. European Journal of Pharmaceutical Sciences: Official Journal of the European Federation for Pharmaceutical Sciences. 2025; 212: 107176. https://doi.org/10.1016/j.ejps.2025.107176.

[18] Liu D, Wu D, Zhao L, Yang Y, Ding J, Dong L, *et al*. Arsenic Trioxide Reduces Global Histone H4 Acetylation at Lysine 16 through Direct Binding to Histone Acetyltransferase hMOF in Human Cells. PloS One. 2015; 10: e0141014. https://doi.org/10.1371/journal.pone.0141014.

[19] Wang M, Mu G, Qiu B, Wang S, Tao C, Mao Y, *et al*. Competitive antagonism of KAT7 crotonylation against acetylation affects procentriole formation and colorectal tumorigenesis. Nature Communications. 2025; 16: 2379. https://doi.org/10.1038/s41467-025-57546-7.

[20] Wei Y, Cai X, Wu Q, Liao H, Liang S, Fu H, *et al*. Extraction, Isolation, and Component Analysis of Turmeric-Derived Exosome-like Nanoparticles. Bioengineering (Basel, Switzerland). 2023; 10: 1199. https://doi.org/10.3390/bioengineering10101199.

[21] Hassan FU, Rehman MSU, Khan MS, Ali MA, Javed A, Nawaz A, *et al*. Curcumin as an Alternative Epigenetic Modulator: Mechanism of Action and Potential Effects. Frontiers in Genetics. 2019; 10: 514. https://doi.org/10.3389/fgene.2019.00514.

[22] Wan X, Wang D. Curcumin: Epigenetic Modulation and Tumor Immunity in Antitumor Therapy. Planta Medica. 2025; 91: 320–337. https://doi.org/10.1055/a-2499-1140.

[23] Song Y, Feng N, Yu Q, Li Y, Meng M, Yang X, *et al*. Exosomes in Disease Therapy: Plant-Derived Exosome-Like Nanoparticles Current Status, Challenges, and Future Prospects. International Journal of Nanomedicine. 2025; 20: 10613–10644. https://doi.org/10.2147/IJN.S540094.

[24] Wei C, Zhang M, Cheng J, Tian J, Yang G, Jin Y. Plant-derived exosome-like nanoparticles - from Laboratory to factory, a landscape of application, challenges and prospects. Critical Reviews in Food Science and Nutrition. 2025; 65: 4510–4528. https://doi.org/10.1080/10408398.2024.2388888.

[25] Raimondo S, Naselli F, Fontana S, Monteleone F, Lo Dico A, Saieva L, *et al*. Citrus limon-derived nanovesicles inhibit cancer cell proliferation and suppress CML xenograft growth by inducing TRAIL-mediated cell death. Oncotarget. 2015; 6: 19514–19527. https://doi.org/10.18632/oncotarget.4004.

[26] Wang Q, Zhuang X, Mu J, Deng ZB, Jiang H, Zhang L, *et al*. Delivery of therapeutic agents by nanoparticles made of grapefruit-derived lipids. Nature Communications. 2013; 4: 1867. https://doi.org/10.1038/ncomms2886.

[27] Heeke S, Gay CM, Estecio MR, Tran H, Morris BB, Zhang B, *et al*. Tumor- and circulating-free DNA methylation identifies clinically relevant small cell lung cancer subtypes. Cancer Cell. 2024; 42: 225–237.e5. https://doi.org/10.1016/j.ccell.2024.01.001.

[28] Yu X, Zhao H, Wang R, Chen Y, Ouyang X, Li W, *et al*. Cancer epigenetics: from laboratory studies and clinical trials to precision medicine. Cell Death Discovery. 2024; 10: 28. https://doi.org/10.1038/s41420-024-01803-z.

[29] Shvedunova M, Akhtar A. Modulation of cellular processes by histone and non-histone protein acetylation. Nature Reviews. Molecular Cell Biology. 2022; 23: 329–349. https://doi.org/10.1038/s41580-021-00441-y.

[30] Wang D, Li H, Chandel NS, Dou Y, Yi R. MOF-mediated histone H4 Lysine 16 acetylation governs mitochondrial and ciliary functions by controlling gene promoters. Nature Communications. 2023; 14: 4404. https://doi.org/10.1038/s41467-023-40108-0.

[31] Zhao K, Zheng M, Su Z, Ghosh S, Zhang C, Zhong W, *et al*. MOF-mediated acetylation of SIRT6 disrupts SIRT6-FOXA2 interaction and represses SIRT6 tumor-suppressive function by upregulating ZEB2 in NSCLC. Cell Reports. 2023; 42: 112939. https://doi.org/10.1016/j.celrep.2023.112939.

[32] Fiorentino F, Sementilli S, Menna M, Turrisi F, Tomassi S, Pellegrini FR, *et al*. First-in-Class Selective Inhibitors of the Lysine Acetyltransferase KAT8. Journal of Medicinal Chemistry. 2023; 66: 6591–6616. https://doi.org/10.1021/acs.jmedchem.2c01937.

[33] Ghorbani-Nejad B, Baghani M, Amiri S, Delche NA, Darijani MH, Soltani M, *et al*. Curcumin: multifaceted biological actions and therapeutic implications-a narrative review. Inflammopharmacology. 2025; 33: 6309–6327. https://doi.org/10.1007/s10787-025-01932-6.

[34] Guo Y, Xu H, Shen P, Cai R. Investigating the Potential of Curcumin in the Treatment of Nonsmall Cell Lung Cancer: A Systematic Review With Meta-Analysis, Network Pharmacology, and Mendelian Randomization. Phytotherapy Research: PTR. 2025; 39: 5062–5084. https://doi.org/10.1002/ptr.70073.

[35] Fonseca R, Louzano YDS, Ortiz CJC, Silva MDF, Felix MLV, Ferreira-Silva GÁ, *et al*. Curcumin-like Compound Inhibits Proliferation of Adenocarcinoma Cells by Inducing Cell Cycle Arrest and Senescence. Pharmaceuticals (Basel, Switzerland). 2025; 18: 914. https://doi.org/10.3390/ph18060914.

[36] Tang C, Liu J, Yang C, Ma J, Chen X, Liu D, *et al*. Curcumin and Its Analogs in Non-Small Cell Lung Cancer Treatment: Challenges and Expectations. Biomolecules. 2022; 12: 1636. https://doi.org/10.3390/biom12111636.

[37] Obeid MA, Alsaadi M, Aljabali AA. Recent updates in curcumin delivery. Journal of Liposome Research. 2023; 33: 53–64. https://doi.org/10.1080/08982104.2022.2086567.

[38] Vitor MT, Bergami-Santos PC, Zômpero RHF, Cruz KSP, Pinho MP, Barbuto JAM, *et al*. Cationic liposomes produced via ethanol injection method for dendritic cell therapy. Journal of Liposome Research. 2017; 27: 249–263. https://doi.org/10.1080/08982104.2016.1196702.